

# A Comparison of Material Removal Mechanism under Low Stress Abrasive Condition of Steel and Hardfacing Alloys

R. Dasgupta, B.K. Prasad, O.P. Modi, and A.K. Jha

(Submitted 28 January 1999; in revised form 9 February 1999)

The low stress abrasive wear behavior of two types of steels commonly used for making a number of commonly used engineering components has been compared with the composition of a few hardfacing alloys that can be overlaid on the steels to impart a wear-resistant surface. The mechanism of material removal as studied by the scanning electron micrographs of the worn and transverse sections is different for the steels and hardfacing alloys. An attempt has been made to explain the mechanism of material removal for the steels and hardfacing alloys.

**Keywords** abrasion, hardfacing alloys, tribology, wear

## 1. Introduction

Wear is essentially a surface phenomenon that can be combated by applying protective coatings (Ref 1-4). There is a wide spectrum of deposition techniques and materials available for depositing such protective layers. The thickness of the layer can vary from micron to millimeter levels. Application of a wear-resistant layer by welding is an economical method and can be employed in areas where thick coatings are required and dimensional tolerances are not very stringent. Another advantage of this technique is that it can be applied on all substrates making the properties of the substrate material irrelevant.

This article compares the low stress abrasive wear properties of two types of steels commonly used in fabricating a number of engineering components with those of a few low chromium (chromium content less than 12%) hardfacing alloys (Ref 5).

## 2. Experimental Details

### 2.1 Materials and Microstructural Analysis

Table 1 gives the compositions for the two types of steels used for the tests. Steel 1 was used for overlaying with three types of low chromium category (Ref 5) hardfacing alloys.

R. Dasgupta, B.K. Prasad, O.P. Modi, and A.K. Jha, Regional Research Laboratory (CSIR), Bhopal (M.P.)-462 026.

The welding electrodes were 3.15 mm in diameter with a thickness of approximately 3000 μm overlaid by manual arc welding.

Samples of approximately 20 by 20 by 8 mm steel and transverse sections of hardfaced steels were metallographically polished using conventional polishing techniques and etched in 0.1% nital solution. The samples were observed under an optical microscope to study the microstructural features of the steels/overlayed material and the bonding between the steel and overlay.

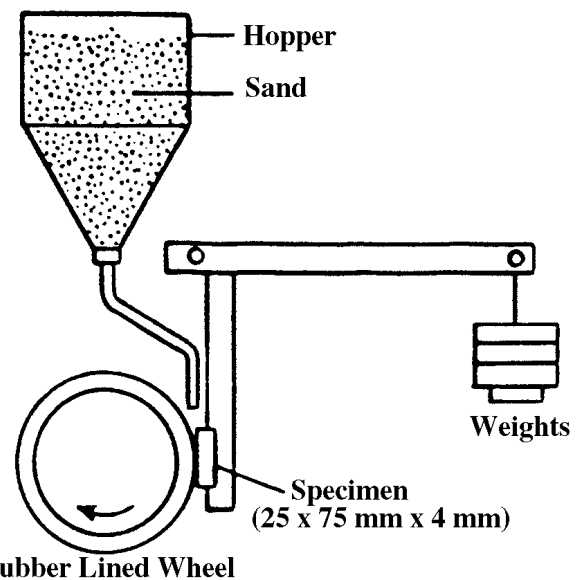


Fig. 1 Schematic diagram of low stress abrasive wear tester

Table 1 Chemical composition and hardness of steels and hardfacing alloys

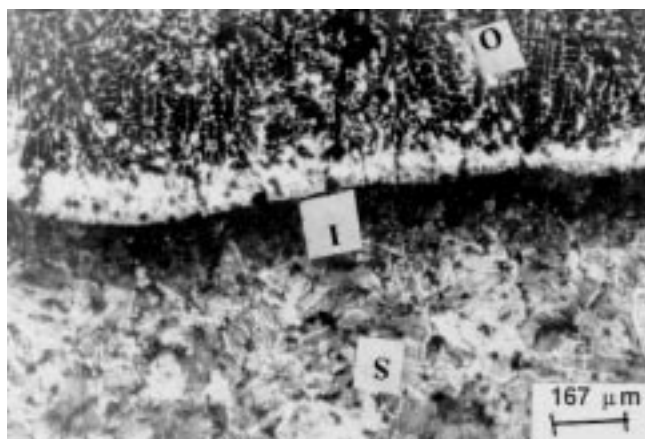
Alloy	Composition, wt%						Hardness, HV
	C	Si	Cr	Mn	Ni	Fe	
Steel 1	0.30	0.06	0.06	0.06	0.06	bal	190 ± 10
Steel 2	0.62	1.65	0.05	0.06	0.13	bal	310 ± 8
HA 1	0.20	0.40	1.80	0.60	...	bal	220 ± 15
HA 2	0.20	0.40	3.20	0.60	...	bal	390 ± 12
HA 3	0.50	0.45	6.50	0.30	...	bal	560 ± 10

HA, hardfacing alloys

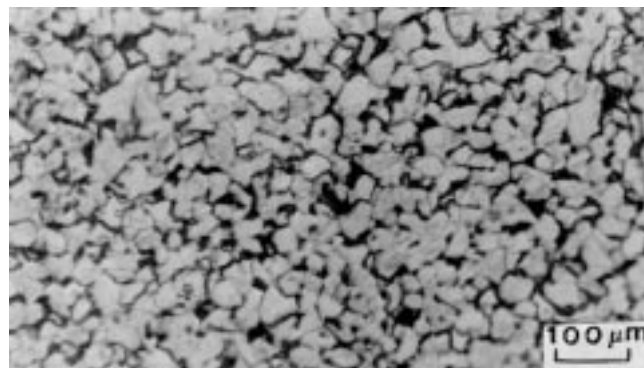
## 2.2 Wear Tests

Low stress abrasive wear tests were carried out on metallographically polished samples of 20 by 70 by 4 mm on a Falex rubber wheel abrasion tester (RWAT) (Falex Corp., Sugar Grove, IL) per ASTM G 65-81 specifications (Ref 6). Figure 1 gives the schematic view of the apparatus. In the test, the test specimen is held against a rotating rubber wheel. Abrasive particles are allowed to fall constantly in between the rotating

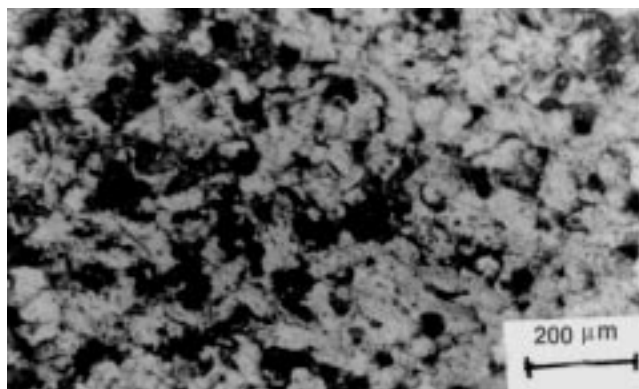
wheel and specimen. In the present study, silica sand between 212 and 300  $\mu\text{m}$  was used as the abrasive, the wheel was rotated at a speed of 273 rpm, and static loads were applied through a cantilever mechanism. Tests were carried out at 22 and 49 N loads. The samples were weighed prior to the test, and weight loss was measured at 2 min intervals, corresponding to a linear traversal distance of 392 m (Ref 6). Tests were carried out up to a linear traversal distance of 5600 m. From the weight loss after every 2 min test duration, volume loss was calculated by dividing the weight loss by the density of the sample. The volume loss was plotted against the sliding distance. The wear rate was



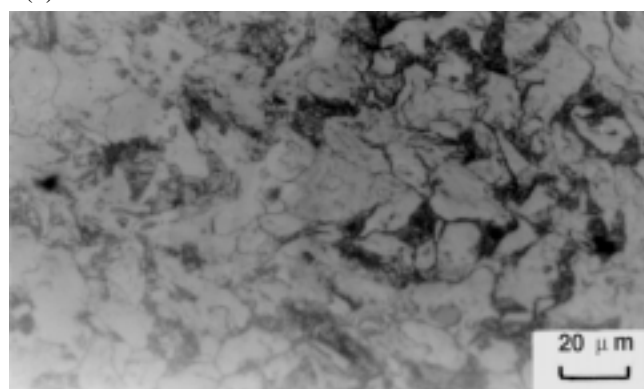
(a)



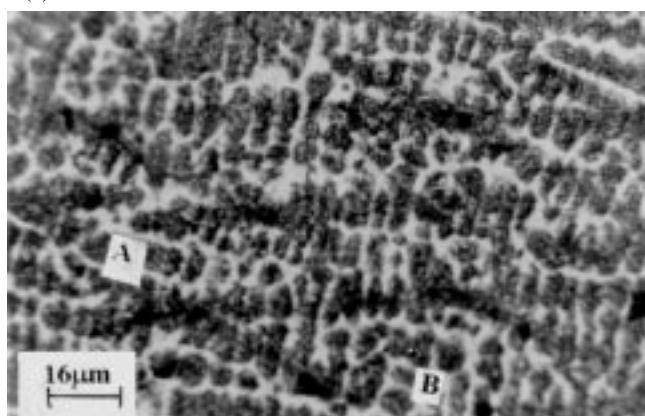
(b)



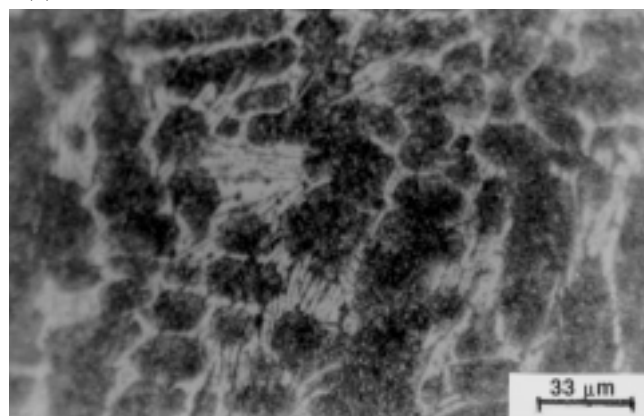
(c)



(d)



(e)



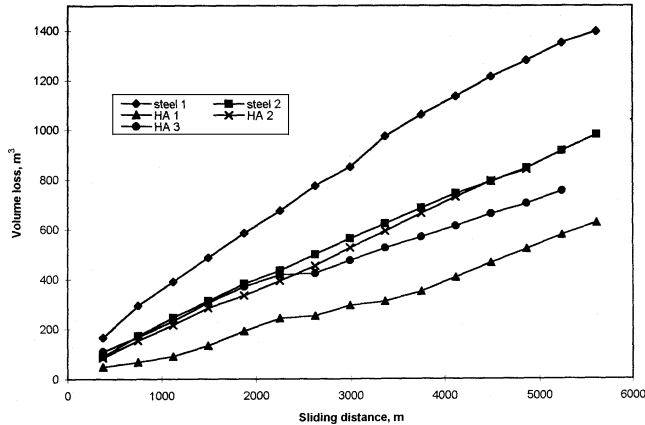
(f)

**Fig. 2** Microstructural features of steels and hardfacing alloys. (a) Bonding between steel and hardfacing alloy showing bonding (I) between substrate (S) and overlay (O). (b) Steel 1. (c) Steel 2. (d) HA 1. (e) HA 2. (f) HA 3

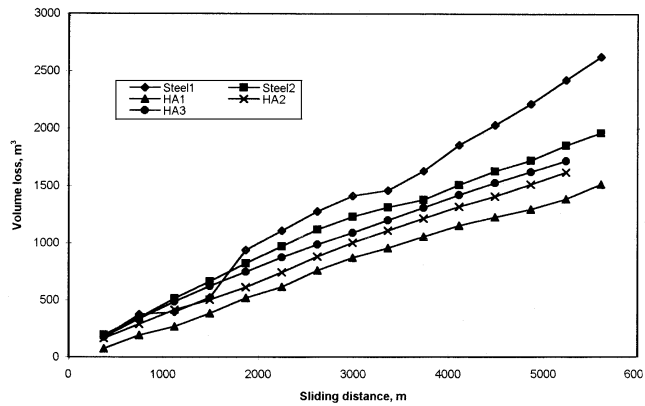
calculated by dividing the volume loss by the distance transversed for the test duration. In the present case, the wear rate was calculated at a sliding distance of 5000 m for all the samples.

### 2.3 Worn and Subsurface Studies

Samples were cut from the worn surface and observed under a scanning electron microscope to study the features. Such



(a)



(b)

**Fig. 3** Variation of volume loss with sliding distance for steels and hardfacing alloys at (a) 22 N load and at (b) 49 N load

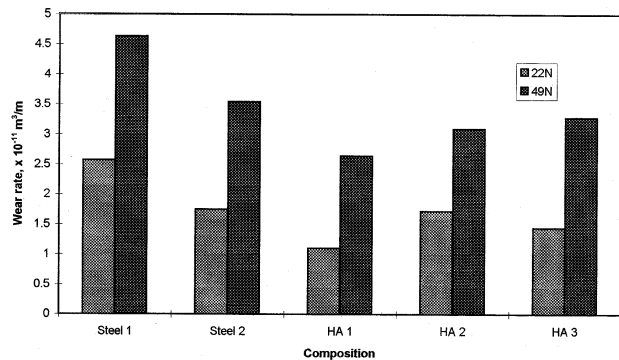


**Fig. 4** Variation of wear rate for different compositions at a sliding distance of 5000 m

studies helped in assessing the effects of material composition microstructural features and the load in the material removal mechanism.

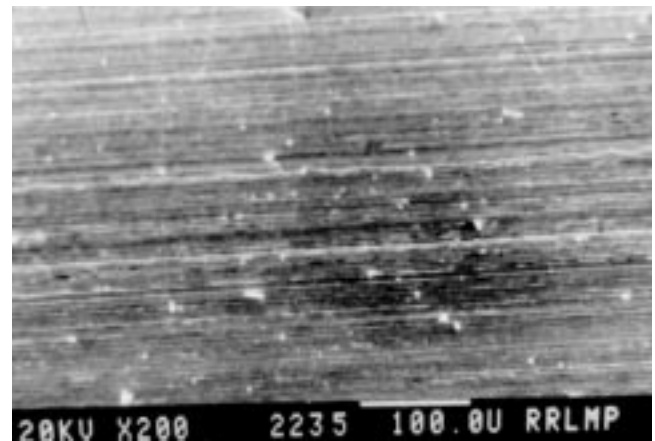
A transverse section of the worn surface was metallographically polished and etched in 0.1% nital to observe microstructural changes (if any), subsurface damage, the affected layer, etc.

## 3. Results

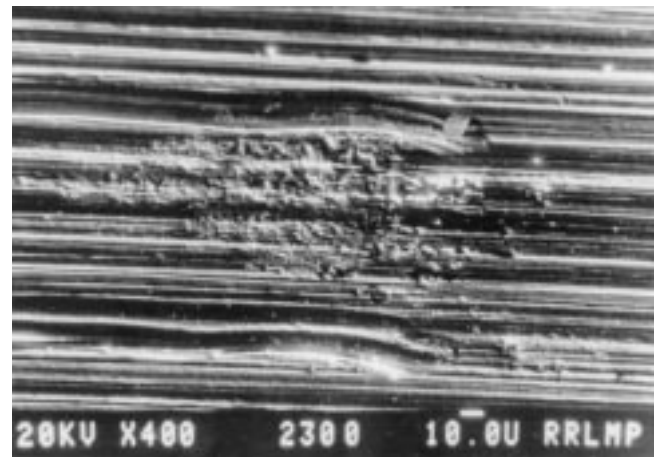
### 3.1 Microstructural Features

The transverse section of the overlaid sample (Fig. 2a) shows a good bonding (I) between the substrate (S) and overlay (O) for the case of overlay composition B. The bonding is similar for the other two compositions also.

The microstructural features of both the steel (Fig. 2b and c) exhibit ferrite and pearlite. The amount of pearlite is more for steel 2 as compared to that of steel 1. The overlay structures are mainly dendritic. The microstructural features of hardfacing alloys HA 1 and HA 2 are similar. The microconstituents are primary austenite and austenite plus carbides in the interdendritic



(a)



(b)

**Fig. 5** Worn surface of steel 1 at (a) 22 N load and at (b) 49 N load

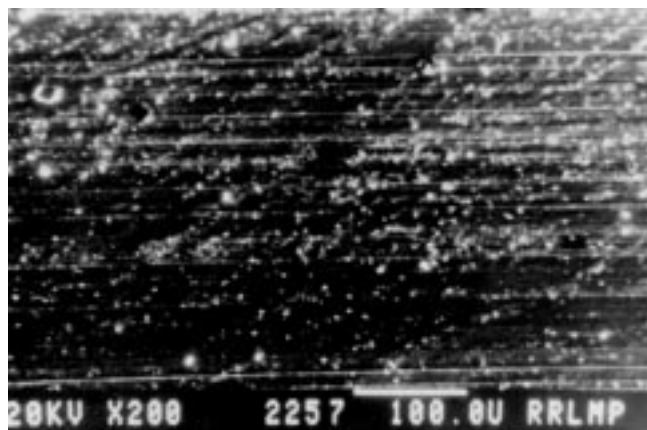
regions (Fig. 2d and e). The HA 2 sample contains more carbide. The microstructure of HA 3 (Fig. 2f) exhibits chromium containing carbides in the dendrites and carbide plus austenite in the interdendritic regions (Ref 7-9).

### 3.2 Wear Behavior

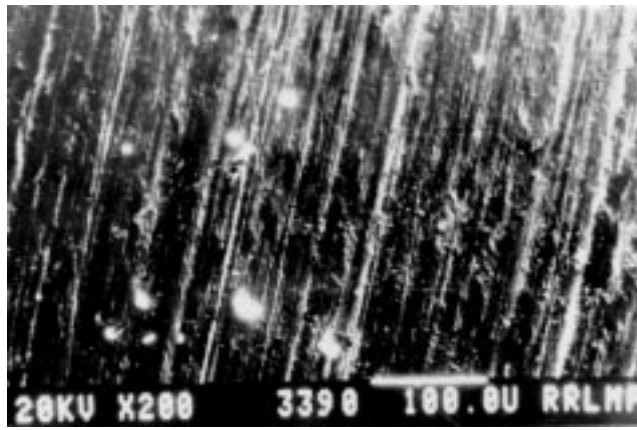
The low stress abrasive wear behavior, that is, volume loss against sliding distance of the steels and hardfacing alloys at 22

and 49 N loads are compared in Fig. 3(a) and (b), respectively. It is seen that in general the volume loss is more at the 49 N load as compared to the 22 N load.

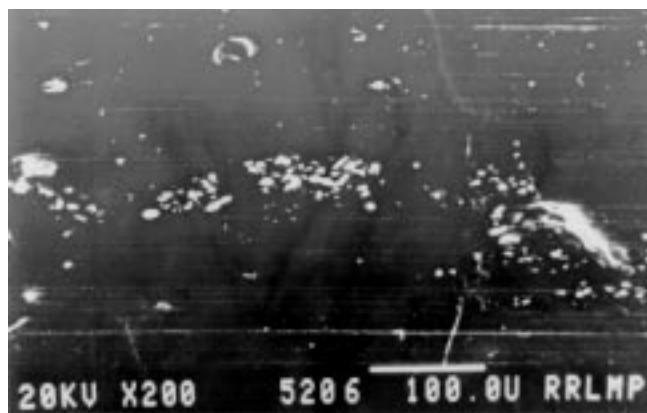
At a load of 22 N, there is a regular increase in volume loss with sliding distance for all the samples. The volume loss for hardfacing alloy composition 3 (HA 3) is the least; for steel 1 the volume loss for hardfacing is maximum throughout the range of sliding distance. Further, the difference between the volume loss for steel 1 and HA 3 increases with sliding dis-



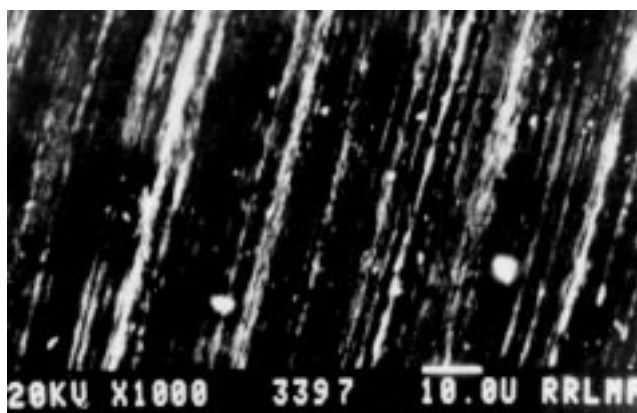
(a)



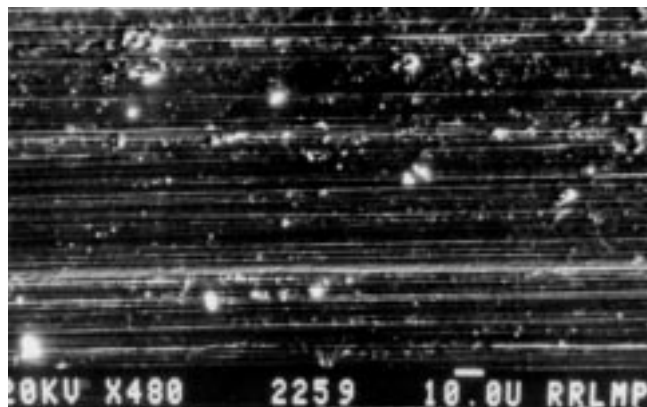
(b)



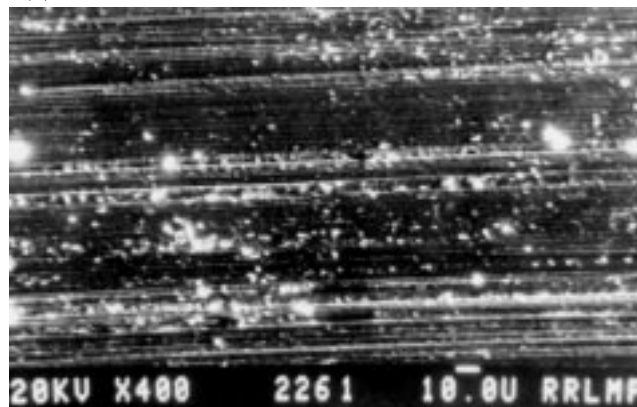
(c)



(d)



(e)



(f)

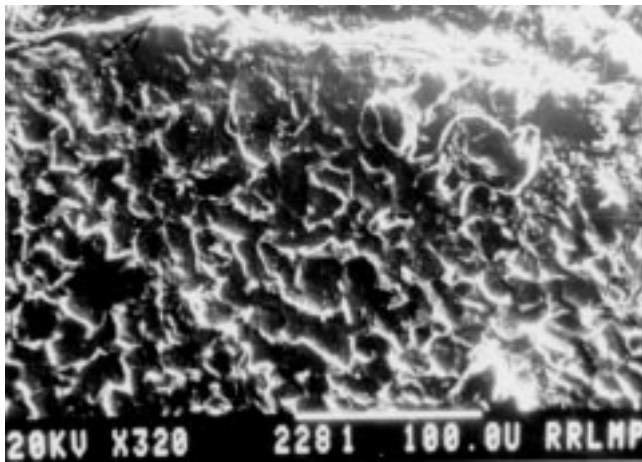
**Fig. 6** Worn surface of hardfacing alloys (a) HA 1 at 22 N, (b) HA 2 at 22 N, (c) HA 3 at 22 N, (d) HA 1 at 49 N, (e) HA 2 at 49 N, and (f) HA 3 at 49 N

tance. There is not much variation in the volume loss between steel 2, HA 1, and HA 2 up to a sliding distance of ~2000 m. But at higher sliding distances the volume loss of HA 1 is significantly less than steel 2 and HA 2. The volume loss for steel 2 and HA 2 is more or less the same for the entire sliding distance tested at a 22 N load.

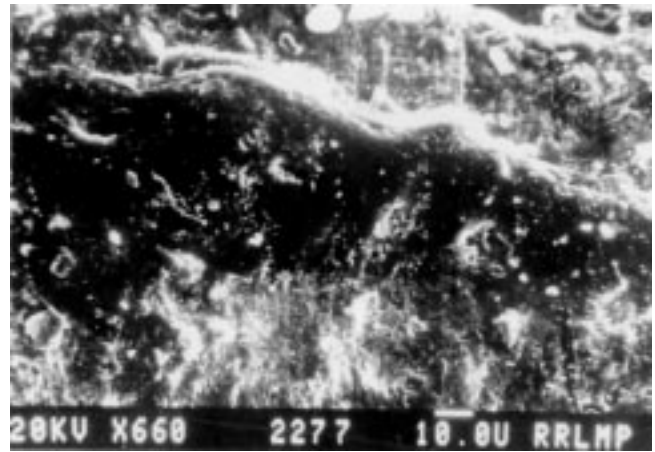
The wear behavior of all the samples at 49 N load is similar to that at 22 N load. Steel 1 exhibits maximum volume loss, and HA 3 exhibits a minimum volume loss. However the volume loss for steel 1 below a sliding distance of ~1500 m is ir-

regular and also lower than that for steel 2 and HA 1. In contrast to the behavior at 22 N load, in this case (that is, at 49 N load) HA 2 shows a lower volume loss than HA 1, which is again lower than steel 2. Thus it is seen that there is an improvement in the performance (as better performance is inversely proportional to the volume loss) of the hardfacing alloys in general for higher loads as compared to the steels.

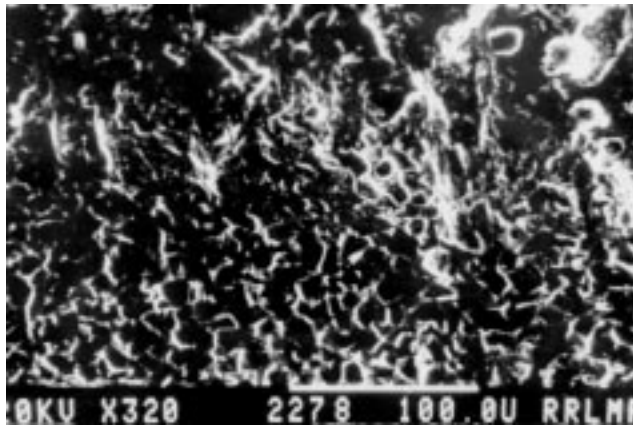
Figure 4 shows the comparative wear rate of the steels and hardfacing alloys at a sliding distance of 5000 m. It is seen that in all the cases wear rate increases with load. The wear rate for



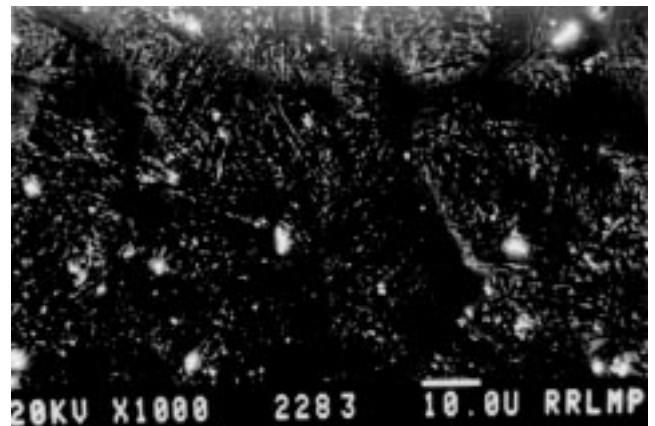
(a)



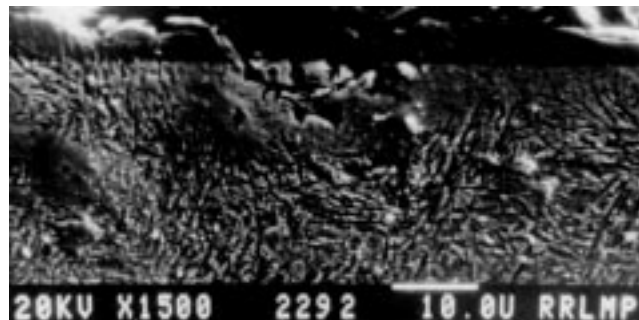
(b)



(c)



(d)



(e)

**Fig. 7** Transverse section of worn surface for steels and hardfacing alloys. (a) Steel at 22 N load showing highly deformed layer. (b) Steel at 49 N load showing similar features as in (a). (c) HA 1 showing coarsening of microstructure below the deformed layer. (d) HA 2. (e) HA 3

HA 3 is the minimum for both the loads, hence its wear resistance (increase of wear rate) is the maximum.

Figure 5 shows the worn surfaces of steel 1 at both the loads. The worn surface at the 22 N load is characterized by continuous grooves and some pitting; as the load is increased to 49 N, the grooves become deeper. Material damage and heavy pitting evidence (marked A) is indicative of severe wear.

Figure 6 shows the worn surfaces of the hardfacing alloys. At 22 N load, the worn surface is characterized by shallow wear grooves. In the case of HA 2 the grooves are the shallowest. At 49 N load, the grooves are quite shallow for HA 3 but deep for the other two compositions. For HA 1, material removal along the wear tracks can also be seen.

Figure 7 shows the transverse section of the worn surfaces for the steels and hardfacing alloys. In the case of steel, a highly deformed layer (marked by arrow in Fig. 7a) can be seen along with some coarsening of the microstructure directly below this layer. Similar features are seen at 49 N load (the deformed layer, Fig. 7b).

For the HA 1 sample, there is a coarsening of the microstructure below the deformed layer (Fig. 7c); such a structure is not visible for HA 2 and HA 3 (Fig. 7d and e).

## 4. Discussion

Material removal under low stress abrasive wear conditions occurs due to material sliding in the presence of loose abrasives (Ref 10). Material removal occurs by micropitting, microcracking, and microploughing. Because wear occurs in the presence of loose abrasives, particle (abrasive) entrapment also occurs. Entrapment of particles and micropitting is associated with ductile materials, microcracking with brittle material, and microploughing with softer materials (Ref 11, 12).

The depth of grooves seen on the worn surface of the steels and hardfacing alloys is commensurate with this volume loss and hardness, which is an important factor affecting wear behavior (Ref 13-15) (Fig. 4). When increasing the load, in some cases (HA 1 and HA 3) the wear grooves and volume loss increase, but in some cases (HA 2) there is no such variation. This is possibly due to the work hardening capability of the HA 2 alloys.

The worn surface for the steel is characterized by severe wear, and the nature of material removal is mainly by microploughing for steels, which is indicative of its soft nature as compared to that of hardfacing alloys.

Microcracking is mainly used for material removal mechanism in hardfacing alloys and is different from the steels (which exhibit microploughing tendency) even at comparative volume

losses. This is indicated by the brittle nature of the former as compared to the latter. The improved wear resistant properties of HA 3 are reflected in the relatively low damage of the worn surface and are possibly due to the presence of chromium carbides in the alloy (Ref 4).

## 5. Conclusions

The following conclusions can be drawn:

- The low stress abrasive wear properties of steels has been compared with three types of low chromium category hardfacing alloys. Studies reveal that with chromium content around 3 wt%, there is no appreciable improvement in the wear properties at low loads. However considerable improvement is seen for the hardfacing alloys at higher loads. However for hardfacing alloys with chromium concentration of 6 wt%, the low stress abrasive wear behavior is superior under all experimental conditions.
- The nature of material removal is different for steels and hardfacing alloys in that the former exhibits a ductile nature and the latter a brittle nature, even at comparative volume losses.

## References

1. C. Nusum, *Proc. Conf. Thermal Spray Process New Ideas and Processes*, ASM International, 1988
2. R.F. Bunshah, *Deposition Technologies for Films and Coatings*, R.F. Bunshah, Ed., Noyes Publications, 1982
3. *Metals Handbook*, Vol 3-4, 8th ed., American Society of Metals, 1972
4. W. Wu and L.T. Wu, *Metall. Mater. Trans. A*, Vol 27, 1996, p 3639
5. *Metals Handbook*, Vol 6, 8th ed., American Society of Metals, 1972
6. "Standard Practice for Conducting Dry Sand Rubber Wheel Abrasive Tests," ASTM Standard G 65-81, 1981
7. R. Dasgupta, B.K. Prasad, A.K. Jha, O.P. Modi, S. Das, and A.H. Yegneswaran, *J. Mater. Eng. Perform.*, Vol 7, 1998, p 221
8. *Metals Handbook*, Vol 7, ASM International, 1991, p 81
9. R. Dasgupta, B.K. Prasad, A.K. Jha, O.P. Modi, S. Das, and A.H. Yegneswaran, *Wear*, Vol 209, 1997, p 255
10. E. Rabinowich, L.A. Dunn, and P.G. Russell, *Wear*, Vol 4, 1961, p 345
11. O. Scheffer and C. Allen, *Tribol. Int.*, Vol 21, 1998, p 127
12. O.P. Modi, B.K. Prasad, S. Das, A.K. Jha, and A.H. Yegneswaran, *Mater. Trans., JIM*, Vol 35, 1994, p 67
13. G.J. Gore and J.D. Gates, *Wear*, Vol 203-204, 1997, p 544
14. M.M. Krushchov and M.A. Balichev, *Friction Wear Machinery*, Vol 19, 1965, p 1
15. L. Larsen-Badse, *Scr. Metall.*, Vol 24, 1990, p 821